Defect-enhanced annealing by carrier recombination in GaAs

D. Stievenard and J. C. Bourgoin
Laboratoire de Physique des Solides, Institut Supérieur d'Electronique du Nord, rue Francois Baës, 59046 Lille Cedex, France
(Received 17 December 1984)

We have performed a systematic study of carrier injection annealing of the defects introduced by electron irradiation in n-type GaAs in the temperature range 300—355 K and with injected current densities ranging from 0.5 to 2 A cm^{-2}. We first observed that the various defects do not anneal in the same fashion as stated in a previous study. We show that, because the associated activation energies decrease continuously as the injected current increases, the model previously proposed for the enhanced annealing in which the enhancement is induced by the energy which is released when a minority carrier is trapped on the defect site cannot apply. However, this enhanced annealing can be quantitatively understood if the annealing is induced by successive changes of the defect charge state when it traps alternatively minority and majority carriers.

I. INTRODUCTION

The fact that changes of a defect charge state, and correlatively carrier trapping on a defect level, can modify the annealing rate has been recognized for a number of years[1] (for a review, see Ref. 2). In GaAs, this phenomenon was first observed in γ-ray-irradiated laser diodes[3] in which the damage is recovered by current injection. Such behavior is apparently a general feature in III-V materials, a result of the strong electron-lattice coupling in such materials since it has later been observed in GaAs,[4,5] GaP,[6,7] alloys,[8] and more recently in InP.[9,10] In GaAs, Lang and Kimerling[11] (LK) studied the annealing rate of the so-called $E3$ defect which is produced by electron irradiation in n-type material and showed that it is proportional to the rate of recombination of electron-hole pairs on the associated level. In their analysis, LK proposed that the driving effect is the liberation of phonons when the defect captures a hole, i.e., the so-called "energy released" mechanism.[2] They argued that this mechanism accounts quantitatively for the variation of the activation energy associated with the annealing of $E3$ since this energy drops from 1.4 eV for thermal annealing to 0.34 eV under injection, i.e., from a quantity equal to the energy liberated by hole trapping on the $E3$ level (situated at 1.1 eV from the valence band). In the case of the defects $E1$ and $E2$, they could not reach the saturation regime in which the rate of trapping is limited by electron and they could not verify quantitatively their model. Moreover, they did not attempt to perform the same study on the other traps ($E4$ and $E5$) present at the same time in irradiated materials. In their discussion, LK also argued that this enhanced annealing is not due to the accompanying change in the average state, i.e., that the annealing is not due to the so-called Bourgoin mechanism (BM). This last mechanism occurs when the equilibrium configuration of a defect in a given charge becomes the saddle point configuration for its migration when its charge state changes, and vice versa. Then, for a defect which migrates this way, it should be possible to induce its mobility in the space-charge region of a junction by applying an alternative bias: Kimerling and Lang[4] attempted this experiment by pulsing a diode at 1.7 MHz; as they did not observe any change in the concentration of the $E3$ defect they concluded that the BM could not be the origin of the annealing. Unfortunately, this experiment proves nothing[12] because using such value of bias frequency, they did not enhance the rate of charge state change as compared to the rate at thermal equilibrium. Indeed, around 100 °C, the capture rate, which should be equal to the emission rate since we are dealing with equilibrium conditions, is $\simeq$25 MHz. We have therefore performed a systematic study of the annealing rates of $E3$, $E4$, and $E5$ for varying injection levels. As we shall see, the main interesting features are (i) the activation energies associated with the annealing rate are not constant as expected in the model proposed by LK but decreases as the injected current density increases and (ii) the concentration of the $E4$ defect is not modified by the injection, as previously stated by LK.

II. EXPERIMENTAL DETAILS

We have studied the n-side (doped with 10^{16} S atoms cm^{-3}) of a p-n junction, developed by vapor phase epitaxy on a n^+ substrate. The defects $E3$, $E4$, and $E5$ were created by 1-MeV electron irradiation, at room temperature, with a flux of 1 μA cm^{-2}, to a total fluence of $\sim 2\times 10^{15}$ cm^{-2}, in such a way that the total defect concentration is $\sim$10% of the free-carrier concentration. The annealing sequences were performed in the following ranges: 300—350 K and 0.5—2.0 A cm^{-2}. In order to avoid a possible thermal effect, i.e., an increase of the temperature of the junction was controlled *in situ*[13] by a measurement of the emission rate of one of the defects. For this, the junction in which the injection takes place is abruptly reverse biased for a few ms, time during which the emission rate of a defect is measured; the temperature is immediately deduced from this rate, since its variation with temperature was previously determined. The uncertainty on the temperature is lower than 2 K.

In order to correlate the annealing rate with the injected carrier density, it is necessary to estimate this density. It is given by[14]

$$\Delta p=(n_i^2/N_D)[\exp(eV/kT-1)] ,$$

where n_i and N_D are, respectively, the intrinsic and the dopant concentrations and V is the forward applied voltage. A current-voltage characteristic is therefore performed at each annealing temperature in order to correlate I, V, and Δp. The above estimation is verified by applying the relation

$$\Delta p=J\tau_p/eL_p ,$$

where J is the current density, τ_p the lifetime of the holes ($\sim 10^{-6}$ s) and L_p their diffusion length ($\sim 10^{-2}$ cm). For the three current densities J used in this study (0.5, 1.3, and 2.0 A cm^{-2}), the concentrations of the injected holes, are respectively, 3×10^{14}, 8×10^{14}, and 1.2×10^{15} cm^{-3}. Finally, the concentrations of the defects were measured using deep level transient spectroscopy (DLTS), using a double-lock-in amplifier to analyze the capacitance transient.[15]

III. EXPERIMENTAL RESULTS

Figures 1 and 2 show a typical evolution of the DLTS spectra for, respectively, the $E3$ and $E4$ and $E5$ defects in the case of an annealing temperature of 330 K and for an injected current density of 0.5 A cm^{-2}. It can be seen that the defect $E4$ does not anneal (this fact is also verified for the extremal conditions of our study, i.e., 2 A cm^{-2} and 355 K). The corresponding variations of the

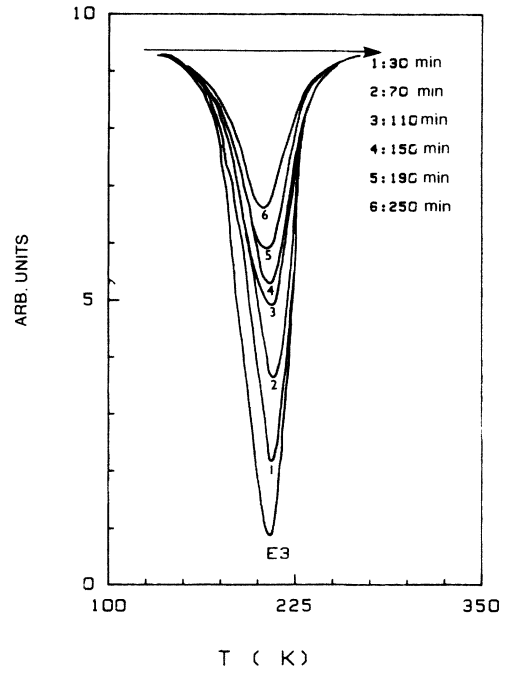

FIG. 1. Evolution of the DLTS spectrum of $E3$ with time of annealing at 330 K for an injected current density of 0.5 A cm^{-2}.

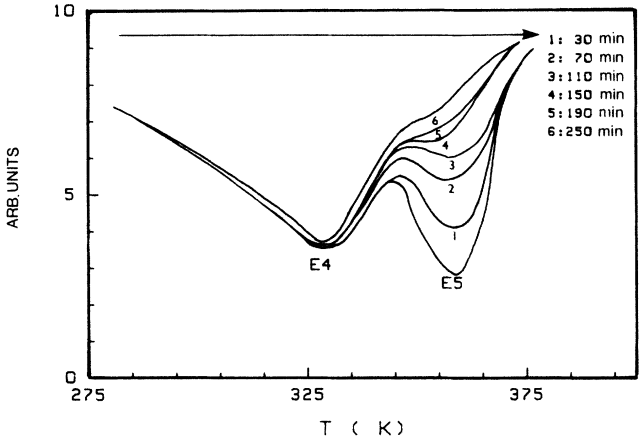

FIG. 2. Evolution of the DLTS spectrum of $E4$ and $E5$ with time of annealing at 330 K for an injected current density of 0.5 A cm^{-2}.

$E3$ and $E5$ concentrations versus the annealing time t are given in Fig. 3. Within the accuracy of the measurement, these concentrations C follow a first-order kinetics given by

$$C=C_0\exp(-\nu t)+C_1 .$$

Indeed, the final concentration C_1 is not zero because a defect labeled $P1$ (Ref. 12) is superposed to $E3$ (then C_1 is the concentration of this defect) and $E5$ appears as a shoulder of the $E4$ peak. Because of this apparent saturation C_1, annealings for very long times were performed ($t\sim30$ h, for instance, at $T\sim355$ K and $J=2$ A cm^{-2}). Figure 4 shows a DLTS spectrum recorded after complete annealing: we can clearly see that $E3$ is transformed to $P1$ and $E5$ just appears as a shoulder of the $E4$ peak. By monitoring the emission rate versus the temperature for the peak left, we verified (Fig. 5) that $E4$ is not modified while $E3$ is replaced by $P1$.

The determination of the annealing rate ν, at each tem-

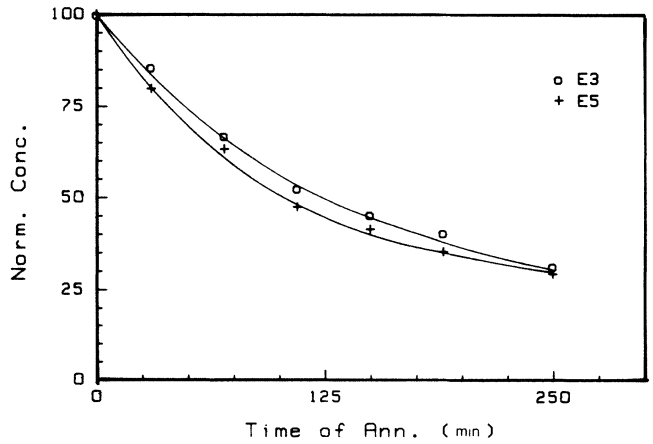

FIG. 3. Variation of the normalized concentrations of $E3$ and $E5$ versus time of annealing at 330 K, for an injected current density of 0.5 A cm^{-2}.

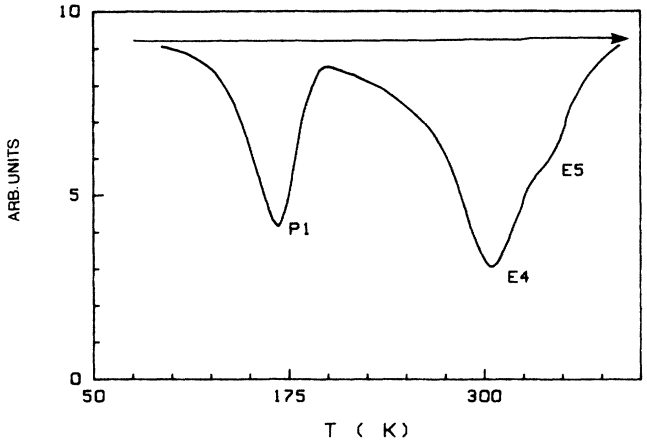

FIG. 4. DLTS spectrum after annealing of 30 h at 355 K with an injected current density of 2 A cm^{-2}.

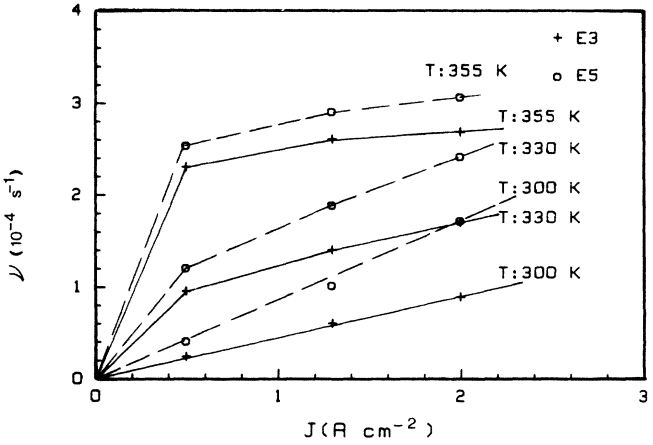

FIG. 6. Variation of the annealing rates of $E3$ and $E5$ versus the injected current density and the temperature.

perature and for each injected current density was made using two techniques: from the measurement of the tangent at $t=0$ and using a numerical fit on the total annealing curve. The variation of ν versus J, for various temperatures, are given in Fig. 6. We have not studied in detail the annealing of the defects $E1$ and $E2$. However, we have performed a DLTS analysis after a 30 h annealing ($\sim$355 K, 2 A cm^{-2}) which shows that the defects have practically not been annealed. Indeed, the ratio of their concentrations to the concentration of $E3$ is about 3 after irradiation,[12] after injection annealing, this ratio is of the order of 30, a value which can be accounted for only by the annealing of $E3$.

We have plotted the values of the annealing rates versus T^{-1} using the injected current density as a parameter on Fig. 7. Clearly, these rates follow an exponential law in which the preexponential factor ν_0 and the activation energy ΔE are functions of J:

$$\nu(J,T)=\nu_0(J)\exp-[\Delta E(J)/kT] .$$

Table I gives the values of $\nu_0(J)$ and $\Delta E(J)$ for the dif-

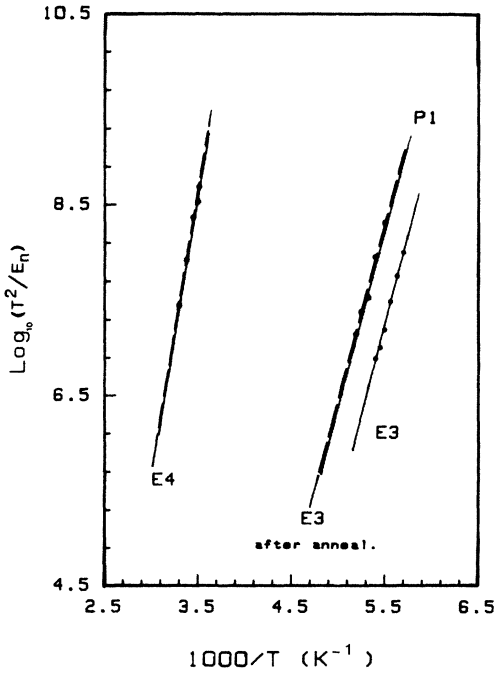

FIG. 5. Signatures of the defects $E3$, $P1$, and $E4$ present before and after long time annealing (30 h, 355 K, 2 A cm^{-2}) ($E3$ with $P1$, $E4$ with $E4$).

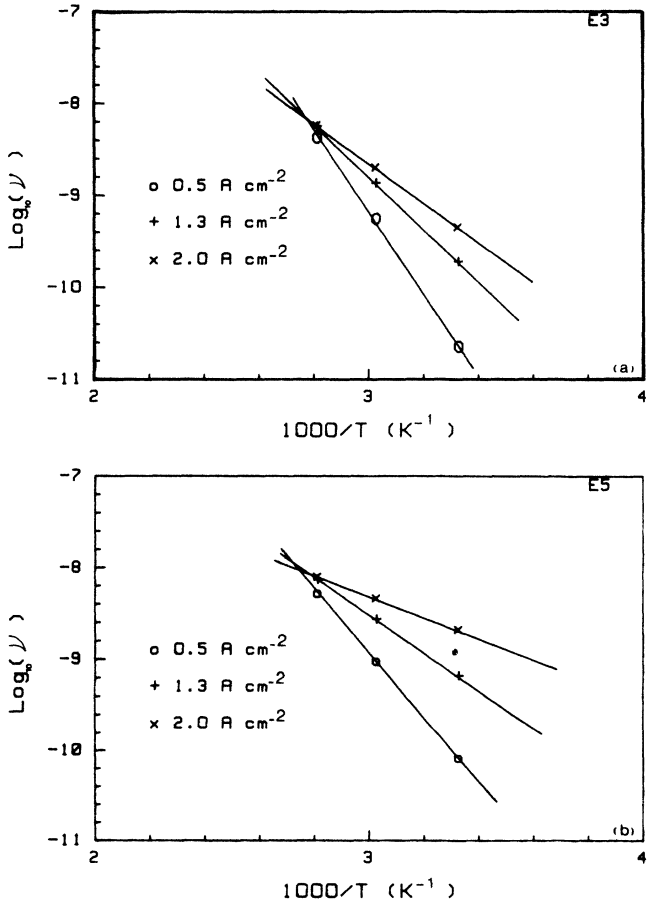

FIG. 7. Variation of the annealing rate ν versus temperature for different densities of injected current for $E3$ and $E5$.

TABLE I. Values of the activation energies (ΔE) and preexponential factors (ν_0) of the defects $E3$ and $E5$ for the various values of the injected current density (J).

J (A cm^{-2})	ΔE_{E3} (meV)	ΔE_{E5} (meV)	$\nu_{0,E3}$ (s^{-1})	$\nu_{0,E5}$ (s^{-1})
0.5	388	307	68.5	5.2
1.3	250	178	0.84	0.09
2.0	188	98	0.12	0.0075

ferent values of J considered.

As shown on Fig. 8 the values of $\Delta E(J)$ are, in practice, linear functions of J for both $E3$ and $E5$ in the range studied. The value of the activation energy determination by KL: $\Delta E_{E3}=340$ meV around 400 K agrees with our results. This particular data corresponds, on the plot $\Delta E(J)$, to a current density of ~ 0.8 A cm^{-2}.

IV. DISCUSSION

A. Rate of charge state change of a defect

During an injection, it is clear that there is a change of the rate at which carriers are trapped on the defects and correlatively a change in the population having a particular charge state. Because the rate of annealing is modified by such injection, it is first interesting to evaluate the corresponding rate of change of charge state of a defect. The dynamics of the rate of change of charge state is given by[16]

$$\frac{db}{dt}=(g_h+k_e)s-(g_e+k_h)b \ , \tag{1}$$

where b and s are the concentrations of filled and empty defects, respectively. The constants k_e and g_e are the capture and emission rates for electrons and k_h and g_h the capture and emission rates of holes.

Using the fraction of occupation β, the above equation reduces to

$$\frac{d\beta}{dt}=(g_h+k_e)(1-\beta)-(g_e+k_h)\beta \ . \tag{2}$$

At equilibrium

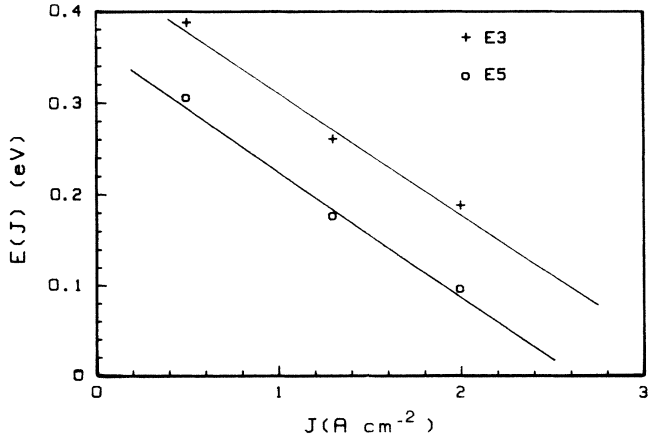

FIG. 8. Variation of the activation energies of $E3$ and $E5$ versus the injected current density.

$$\frac{d\beta}{dt}=0 \tag{3}$$

and

$$\beta=\frac{g_h+k_e}{g_e+k_h+g_h+k_e} \ . \tag{4}$$

The occupancy of a state is obtained by a continual succession of transitions. The rate of change of the charge state (Γ) of a defect is thus obtained by taking the rate of change in a given state (i.e., k_h+g_e for b, k_e+g_h for s) times the probability of finding this state ($1-\beta$ for s, β for b), and summing over all possible states.

Therefore,

$$\Gamma=(g_e+k_h)\beta+(g_h+k_e)(1-\beta) \ . \tag{5}$$

Taking the value of β given in (4), we have

$$\Gamma=2\frac{(k_e+g_h)(g_e+k_h)}{(g_e+k_h)+(g_h+k_e)} \ . \tag{6}$$

The different rates are given by

$$k_e=\sigma_e V_e n \ , \tag{7}$$

$$g_e=\sigma_e\gamma_e T^2\exp\left[-\frac{E_C-E_T}{kT}\right] , \tag{8}$$

$$k_h=\sigma_p V_p P \ , \tag{9}$$

$$g_h=\sigma_p\gamma_p T^2\exp\left[-\frac{E_T-E_V}{kT}\right] , \tag{10}$$

where V_e and V_p are the thermal velocities, γ_e and γ_p constants relative to the semiconductor ($\gamma_e=2.28\times10^{20}$ cm^{-2}s^{-1}K^{-2}, $\gamma_p=1.7\times10^{21}$ cm^{-2}s^{-1}K^{-2} for GaAs), σ_e and σ_p the carrier cross sections, and E_T is the level position of the defect in the gap. Under injection of Δn and Δp carriers, the carrier concentrations to be considered for a n-type material ($n,p=0$) are $n+\Delta n,\Delta p$. In the case of the defects considered and at the temperature where the annealing is performed the generation rates are negligible in front of the corresponding capture rates, i.e., $k_e \gg g_h$ and $k_h \gg g_e$ (see Table II), and Γ reduces to

$$\Gamma=2\frac{k_e k_h}{k_e+k_h} \ . \tag{11}$$

In order to evaluate the hole rate, it is necessary to know the corresponding cross sections. They are known for electron trapping;[12] as for hole trapping, they are deduced from this study, as shown below.

Thus, in the case of a low injection density, $k_h \ll k_e$ and

TABLE II. Values of the various parameters (see text) allowing calculation of the capture and emission rate for the defects $E3$ and $E5$ at 330 K for an injected current density of 0.8 A cm^{-2}.

	$E3$	$E4$	$E5$
E_C-E_T (eV)	0.30	0.76	0.96
E_T-E_V (eV)	1.1	0.64	0.44
γ_e (cm^{-2} s^{-1} K^{-2})	2.28×10^{20}	2.28×10^{20}	2.28×10^{20}
γ_p (cm^{-2} s^{-1} K^{-2})	1.7×10^{21}	1.7×10^{21}	1.7×10^{21}
V_n (cm s^{-1})	3×10^{7}	3×10^{7}	3×10^{7}
V_p (cm s^{-1})	10^{7}	10^{7}	10^{7}
σ_e (cm^2)	$\sim10^{-14}$	$\sim10^{-14}$	$\sim2\times10^{-12}$
σ_p (cm^2)	$\sim10^{-12}$	$\sim10^{-12}$	$\sim2\times10^{-10}$
Δ_p (cm^{-3})	5×10^{14}	5×10^{14}	5×10^{14}
n (cm^{-3})	10^{16}	10^{16}	10^{16}
T (K)	330	330	330
k_e (s^{-1})	3×10^{9}	3×10^{9}	6×10^{11}
g_h (s^{-1})	3×10^{-3}	3×10^{4}	7×10^{9}
k_h (s^{-1})	5×10^{9}	5×10^{9}	10^{12}
g_e (s^{-1})	7×10^{6}	1	10^{-1}

$$\Gamma\simeq 2k_h=2\sigma_p\Delta p(J)V_p\ . \tag{12}$$

Γ varies therefore linearly with J.

When J is large, $k_h\gg k_e$, and Γ reduces to

$$\Gamma\sim 2k_e=2\sigma_n V_n n\ ,$$

and Γ saturates with the current density. Experimentally, the saturation is not complete: a weak increase of the annealing rate versus J is still observed. This is due to the fact that n is not constant but varies as $n+\Delta n(J)$.

The particular point X where the linear variation of Γ with J reaches the saturation regime is given by the relation

$$\sigma_e V_e n=\sigma_p V_p p\ .$$

Because the annealing rate ν follows the same variation as Γ versus J, we use the curves $\nu(J)$ to determine the point X and to evaluate σ_p. For the defect $E3$, we found $(1.7\pm0.5)\times10^{-15}$, $(5\pm1.2)\times10^{-15}$, and $(1.4\pm0.2)\times10^{-14}$ cm^2 at, respectively, 300, 330, and 355 K. These values follow a law

$$\sigma_p=\sigma_{p\infty}\exp(-\Delta E_p/kT)$$

with $\Delta E_p=0.33\pm0.075$ eV and $\sigma_{p\infty}\sim5\times10^{-10}$ cm^2.

B. Rate of annealing

We have first to consider the relation between the annealing rate ν and the rate of charge state change Γ. It is well known (see, for instance, Ref. 17) that kinetics of annealing describing the evolution with time of a defect concentration N can be written as

$$N(t)=N_0e^{-\nu t}\ , \tag{13}$$

where the annealing rate ν is a diffusion coefficient D times a geometrical factor β. The diffusion coefficient is, for a tetrahedral lattice, a jump frequency times a coefficient: $(\frac{1}{8})a^2f$ (where a is the lattice parameter, 5.65 Å for GaAs, and f the correlation factor of 0.5). As to the geometrical factor β, it depends upon the specific phenomenon by which the annealing takes place. Since, in the case considered here, the jump frequency is Γ, the ratio between Γ and the annealing rate ν is the product βD. Figure 9 ($\Delta E_n=0.08$ eV, $\sigma_{n\infty}=3\times10^{-15}$ cm^2, $\Delta E_p=0.30$ eV, $\sigma_{p\infty}=1\times10^{-9}$ cm^2, $n=10^{16}$ cm^{-3}, $V_n=3\times10^7$ cm s^{-1}, $V_p=10^7$ cm s^{-1}) shows a simulation of $\Gamma(J,T)$ for the defect $E3$, which shows that the shape of $\Gamma(J,T)$ is indeed the same as that of ν, providing values of βD given for all data in Table III, i.e., an average value $\beta D=(1.6\pm0.4)\times10^{12}$. (This incertanty on βD, i.e., on Γ, is explained by the incertainty on σ_e.)

C. Activation energy of the annealing

From the plot $\beta D\Gamma(T)$ for the three values of J considered (i.e., 0.5, 1.3, and 2 A cm^{-2}), we can determine the activation energy associated with annealing: it is 0.25, 0.19, and 0.16 eV, respectively. It is decreasing with J as observed experimentally.

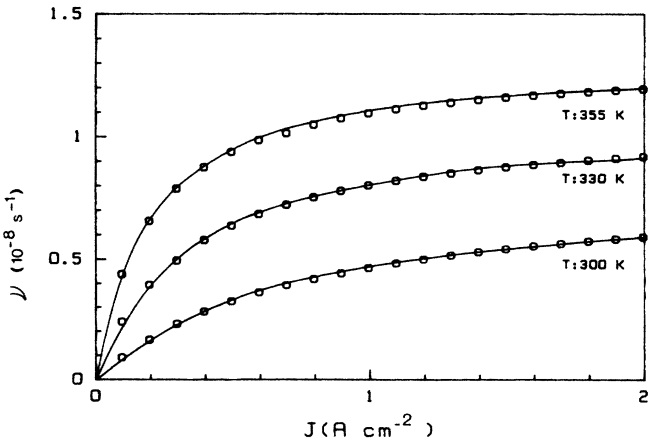

FIG. 9. Simulation, for the defect $E3$, of the rate of change of charge state versus J and T.

TABLE III. Values of the ratio ν/Γ (βD) associated with the defect $E3$ measured for the different temperature (T) and injected current density (J).

	J (A cm^{-2})		
T (K)	0.5	1.3	2
300	0.7×10^{-12}	1.1×10^{-12}	1.4×10^{-12}
330	1.4×10^{-12}	1.6×10^{-12}	1.8×10^{-12}
355	2.4×10^{-12}	2.2×10^{-12}	2.2×10^{-12}

D. The annealing mechanism

LK explained their simple experimental result, namely that the variation of the activation energy between the thermal E_t and the injection E_i annealings, is equal to $E_t-E_i=E_T-E_V$, by the energy released mechanism, in which the energy released by hole trapping on the defect site is used to enhance the annealing. Such a model implies necessarily that the activation energy measured in injection condition remains constant in the saturation regime.

Unfortunately, this is not the case as we have seen when measurements of annealing rates are performed versus T and J. This cannot be explained by the fact the saturation regime is not reached or not complete because, in no way can the energy release mechanism proposed by LK be associated with an activation energy lower than $E_t=(E_T-E_V)$ as we observe. (The apparent activation energy in the nonsaturation regime must be larger than in the saturation regime since the annealing rate is slower.) For instance, for $E3$, $E_t=1.4$ eV, $E_T-E_V=1.1$ eV so, $E_i\sim0.30$ eV; for $E5$, $E_t=1.4$ eV, $E_T-E_V=0.44$ eV, so $E_i\sim0.96$ eV, but we get for $J=2$ A cm^{-2} $E_i(E3)=0.19$ eV, $E_i(E5)=0.10$ eV.

Such variations of E_i versus J cannot be accounted for by the fact that the saturation regime is not reached (for $E5$), or not completely reached (for $E3$), because the annealing rates we observe are already faster than the ones expected in the energy release mechanism. Therefore, we are led to look for another mechanism. This other mechanism, because it must be related to the recombination rate, can only be the one associated with alternative charge state changes the defects undergo under injection (i.e., the so-called BM).

We have still to discuss the reason why some of the defects do not anneal under injection, i.e., $E1$, $E2$, $E4$, and $P1$. This last defect is certainly a complex one, which does not anneal thermally together with the E defects. The difference is annealing behavior is presumably a consequence of this difference of nature. For the others, which are associated with a distribution of vacancy-interstitial pair in the As sublattice,[12] βD is certainly the same. Since ν is negligible for them, the only explanation is that these defects have a capture cross section σ_p very small.

V. CONCLUSION

We have performed a systematic study of the injection annealing for the defects $E3$, $E4$, and $E5$ produced by electron irradiation in n-type GaAs, which are associated with vacancy-interstitial pairs. We have shown that the annealing rate varies with the injected current density J as $\nu_0(J)\exp[-\Delta E(J)/kT]$, where the activation energy is a linear decreasing function of J, for the defects $E3$ and $E5$, whereas $E4$ does not anneal. The variation of the associated activation energy $\Delta E(J)$ with J cannot be explained by the energy released mechanism proposed by Lang and Kimerling. We have demonstrated that only the socalled Bourgoin Mechanism, i.e., the migration induced by alternative changes of the defect charge state can explain quantitatively all experimental observations.

ACKNOWLEDGMENT

This work was supported by Centre National d'Etudes des Télécommunications under Contract No. C84 6B 035. The Laboratoire de Physique Solides is "Laboratoire associé au Centre National de la Recherche Scientifique No. 253."

[1] J. C. Bourgoin and J. W. Corbett, IEEE Trans. Nucl. Sci. **NS-18**, 11 (1971).
[2] J. C. Bourgoin and J. W. Corbett, Radiat. Eff. **36**, 157 (1978).
[3] C. E. Barnes, Phys. Rev. B 1, 4735 (1970).
[4] L. C. Kimerling and D. V. Lang, in *International Conference on Lattice Defects in Semiconductors, Frieberg, Germany, 1974* (IOP, London, 1975), p. 589.
[5] D. V. Lang, L. C. Kimerling, and S. Y. Leung, J. Appl. Phys. **47**, 3587 (1976).
[6] D. V. Lang and L. C. Kimerling, Appl. Phys. Lett. **28**, N5 (1976).
[7] C. Werkhoven, J. H. T. Hengst, and C. van Optorp, Appl. Phys. Lett. **35**, 136 (1979).
[8] M. Ettenberg and C. J. Nuese, J. Appl. Phys. **46**, 2137 (1975).
[9] A. Sibille, in *Proceedings of the 13th International Conference on Defects in Semiconductors,* edited by L. C. Kimerling and J. M. Parsev Jr. (AIME, Warrendale, Penn., 1984), p. 1155.
[10] J. L. Benton, M. Levinson, A. T. Macrauder, H. T. Temkin, and L. C. Kimerling, Appl. Phys. Lett. **45**, 566 (1984).
[11] D. V. Lang, and L. C. Kimerling, Phys. Rev. Lett. **35**, 22 (1975).
[12] D. Pons, and J. C. Bourgoin, J. Phys. C **18**, 3839 (1985).
[13] D. Stievenard and J. C. Bourgoin (unpublished).
[14] S. M. Sze, *Physics of Semiconductors Devices* (Wiley, New York, 1981), p. 84.
[15] D. Pons, P. M. Mooney, and J. C. Bourgoin, J. Appl. Phys. **51**, 2038 (1980).
[16] M. Lannoo and J. C. Bourgoin, *Point Defects in Semiconductors I, Theoretical Aspects* (Springer-Verlag, Berlin, 1981), Chap. 7.
[17] J. C. Bourgoin and M. Lannoo, *Point Defects in Semiconductors II, Experimentals Aspects* (Springer-Verlag, Berlin, 1983), Chap. 9.